

Spin Tunneling in Magnetic Molecules: Quasisingular Perturbations and Discontinuous $SU(2)$ Instantons

Ersin Keçecioglu and Anupam Garg*

Department of Physics and Astronomy,

Northwestern University, Evanston, Illinois 60208

(Dated: October 23, 2018)

Abstract

Spin coherent state path integrals with discontinuous semiclassical paths are investigated with special reference to a realistic model for the magnetic degrees of freedom in the Fe_8 molecular solid. It is shown that such paths are essential to a proper understanding of the phenomenon of quenched spin tunneling in these molecules. In the Fe_8 problem, such paths are shown to arise as soon as a fourth order anisotropy term in the energy is turned on, making this term a singular perturbation from the semiclassical point of view. The instanton approximation is shown to quantitatively explain the magnetic field dependence of the tunnel splitting, as well as agree with general rules for the number of quenching points allowed for a given value of spin. An accurate approximate formula for the spacing between quenching points is derived.

PACS numbers: 03.65.Db, 75.10Dg, 03.65.Sq, 03.65.Xp

*e-mail address: agarg@northwestern.edu

I. INTRODUCTION

A. Overview

Among the several advances in the study of large-spin molecular magnets in the last few years [1], perhaps the most remarkable is the observation of quenching of spin tunneling in the molecule $[\text{Fe}_8\text{O}_2(\text{OH})_2(\text{tacn})_6]^{8+}$ (or just Fe_8 for brevity) by Wernsdorfer and Sessoli (WS) [2, 3]. The spin of this molecule can tunnel between classically degenerate orientations, but for certain values of the applied magnetic field, it is found that the tunneling is eliminated, or quenched. Between quenching points, the tunnel splitting oscillates as a function of applied field. The simplest model that is capable of describing this effect has been studied by many workers now [4, 5, 6, 7, 8, 9, 10, 11], and it is well understood qualitatively in terms of an interference between tunneling Feynman paths. Such interference can also arise for massive particles in more than one dimension [12]. It arises in the case of a single spin because the kinetic term in the path integral has a geometrical or Berry phase structure [4, 13, 14].

There is, however, yet another aspect of the Fe_8 experiments that has not been widely appreciated, because of which the physical explanation for the tunnel splitting oscillations is significantly incomplete. This is because if we view the tunneling in terms of just the interfering paths, the geometrical interpretation of the relative phase between them inevitably predicts a certain number — ten — of quenching points. Experimentally, and by numerical diagonalization of the appropriate model Hamiltonian, only four quenching points are seen. We will show in this paper that the resolution of this apparent paradox requires that we include paths that have *discontinuities* at the end points. As a general point, the necessity of including such paths in the spin-coherent-state path integral has in fact been known for some time [15, 16], but the significance of this idea has not progressed much beyond the purely formal level, and the one concrete problem where discontinuous paths are known to be needed — Larmor precession in a constant magnetic field — is so well understood to begin with, that few people have pursued this line of inquiry further. The Fe_8 problem has provided us with a strong motivation for doing just that, thus enhancing our understanding of the spin-coherent-state path integral. In turn, we can now see that discontinuous paths exist in all other coherent-state path integrals too, and this may prove to be of use in situations where such path integrals are the natural analytic tool.

There are, therefore, two points to this paper. First, as already stated, is to advance our understanding of the spin-coherent-state path integral. Second, we obtain a *quantitative* analytical explanation for additional aspects of WS's data that are not captured by the simple model, and that have up till now been only understood numerically. This is desirable as the oscillations seen in Fe_8 are, to date, the clearest evidence for spin tunneling of a spin of such large magnitude.

This may be a good point to ask why one should bother with an analytical explanation at all. After all, the model Hamiltonian (1.4) given below can be numerically diagonalized with minimal effort. A numerical diagonalization by itself gives no insight into the results, however, and if it were the only way we had of solving the problem, the oscillations in the splitting would be a complete mystery. If one believes that the mental picture of interfering tunneling paths is useful, then it is surely important to know if and when and how this picture breaks down. Secondly, the numerical approach cannot by itself explain the scale of the tunnel splitting.

A shorter paper with our results has been published previously [17]. In the present paper, in addition to providing the details of the work, we explain how to find the end points of the discontinuous paths or boundary jump instantons, as we refer to them. We also discuss the general model for parameter values other than those relevant to Fe_8 in order to further test the scenario for the elimination of quenching points. Finally, we show that the number of quenching points that remain must be even or odd depending on the value of the spin, J , and how this comes about from the instanton analysis.

B. Basic Facts about Fe_8

The main facts about Fe_8 are as follows. The cluster of eight Fe^{3+} ions in one molecule has an approximate D_2 symmetry. Competing exchange interactions among the ionic spins in one molecule lead to a ground state with a total spin of $J = 10$. The compound forms a well ordered crystalline solid, in which the magnetic ions in one molecule are kept well separated from those in another molecule by large organic ligands. The magnetic degrees of freedom may thus be treated as a set of non-interacting spins, each with $J = 10$. To a first approximation, the anisotropy of each molecule may be described by the Hamiltonian

$$\mathcal{H}_0 = -k_2 J_z^2 + (k_1 - k_2) J_x^2 - g\mu_B \mathbf{J} \cdot \mathbf{H}. \quad (1.1)$$

TABLE I: Important parameter combinations

Quantity	Formula
H_c	$2k_1J/g\mu_B$
λ	k_2/k_1
λ_2	CJ^2/k_1
h	H/H_c
ζ	$4\lambda_2h^2$

Here, g is the gyromagnetic ratio, μ_B is the Bohr magneton, and $k_1 > k_2 > 0$ are anisotropy parameters. Equation (1.1) is the simplest Hamiltonian that can describe the quenching effect. Viewed as a classical Hamiltonian, it has two degenerate ground states at the points $\mathbf{J} = \pm J\hat{\mathbf{z}}$ in the absence of an applied field. These states are separated by a barrier k_2J^2 along the y -axis, and k_1J^2 along the x -axis. Quantum mechanics admixes these states via tunneling [18]. When the field is non-zero, the classical minima are no longer along $\pm\hat{\mathbf{z}}$, but they are still degenerate if $\mathbf{H} \perp \hat{\mathbf{z}}$, the easy axis, and one can have tunneling between the corresponding quantum mechanical states. More generally, one can have tunneling between excited states in the two wells. In this paper, however, we will only consider $\mathbf{H} \parallel \hat{\mathbf{x}}$, and tunneling between the lowest two states. In this case, the quenching points are perfectly regularly spaced, and are located at

$$H_x = (J - n - \frac{1}{2})\Delta H_x^{(0)}, \quad n = 0, 1, \dots, 2J - 1, \quad (1.2)$$

where the spacing or period is given by

$$\Delta H_x^{(0)} = \frac{\sqrt{1 - \lambda}}{J} H_c, \quad (1.3)$$

where $\lambda = k_2/k_1$, and $H_c = 2k_1J/g\mu_B$. (These, and other important parameter combinations are tabulated in Table I.)

We note in passing that although this and similar results for other quenching points were initially obtained by various semiclassical approximations [4, 5, 7], they are in fact exact [19] for the model (1.1).

WS's observations differ from the simple model predictions in that they see only four quenching points on the positive H_x axis, where the simple model would say ten, and the

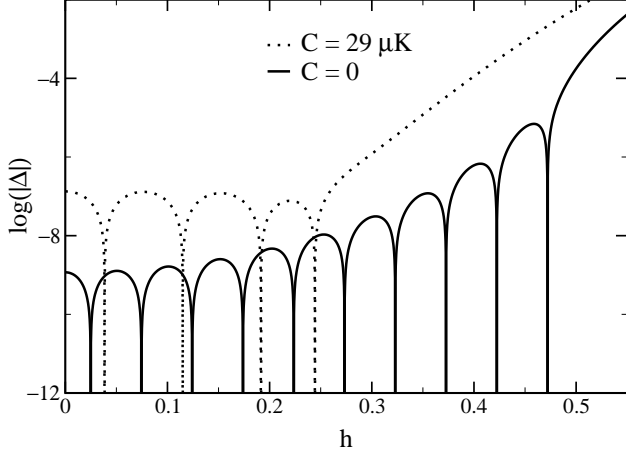


FIG. 1: Tunnel splitting Δ between the ground level pair for the Hamiltonian (1.4) with $C = 0$ (solid line) and $C = 29 \mu\text{K}$ (dotted line). Plotted is $\log_{10} |\Delta|$, with Δ measured in Kelvin.

spacing between these points is more than 50% greater than the formula (1.3) would give. (See Fig. 1.) At the same time, this spacing is quite uniform. They surmise that the differences are due to the presence of higher order anisotropy terms in the Hamiltonian consistent with the symmetry of the molecule, and by trial and error and numerical diagonalization of a 21×21 matrix, they discover that their data can be very well fit by the following model Hamiltonian [20]

$$\mathcal{H} = -k_1 J_z^2 + (k_1 - k_2) J_x^2 - C[J_+^4 + J_-^4] - g\mu_B \mathbf{J} \cdot \mathbf{H}. \quad (1.4)$$

The parameters g , k_1 and k_2 are known through a variety of experimental evidence [21, 22, 23, 24]. We will use the values used by WS: $g \simeq 2$, $k_1 \simeq 0.338$ K, $k_2 \simeq 0.246$ K, and $C = 29 \mu\text{K}$. It turns out to be important that one needs $C > 0$.

This, then, describes the problem that we wish to solve. One point to note is that the dimensionless strength of the fourth order anisotropy C is

$$\lambda_2 = CJ^2/k_1. \quad (1.5)$$

For the Fe_8 parameter values, $\lambda_2 = 8.580 \times 10^{-3}$. That such a small term should have such a large effect (elimination of six quenching points, 50% increase in period), suggests that it is a singular perturbation. We shall see that this is indeed true when we analyze its effect on the semiclassical paths, although the perturbation is perfectly well behaved from the quantum mechanical operator point of view.

C. Plan of paper

The plan of the paper is as follows. In Sec. II we briefly review the formalism of SU(2) instantons with special emphasis on the jump instantons. To this end, we first discuss (Sec. II A) stereographic coordinates for the unit sphere, the corresponding parametrization of spin coherent states, and how paths on the complexified unit sphere are represented in terms of stereographic as well as the usual spherical polar coordinates. We then discuss (Sec. II B) the action functional for spin, and show that unless one includes a “boundary term” that depends explicitly on the boundary values of the spin path, there is no sensibly formulatable least action principle, nor is there a solution to the Euler-Lagrange equations in general. Paths with discontinuities arise naturally once a boundary term is included. We also discuss Klauder’s formulation of these points in terms of an extra infinitesimal pseudo-inertial term in the kinetic energy and the concomitant production of narrow boundary layers in the spin paths. In the limit where the extra kinetic energy term vanishes, the width of these layers also vanishes, and they then look like discontinuities in the paths.

In Sec. II C, we discuss the general structure of the tunnel splitting for the model (1.4) when both types of instantons—with and without jumps—are allowed. We shall see that an instanton of the latter type dominates as the field gets large, and since this instanton has no interfering partner, we see why the splitting ceases to oscillate after fewer than ten quenching points have been realized.

In Sec. III we present the explicit analysis for our model for Fe₈, Eq. (1.4). In Sec. III A we analyse the interfering instantons. We identify $\zeta = 4\lambda_2 h^2$ (with $h = H/H_c$) as the appropriate small parameter, and explain why the H_x spacing of the quenching points is so regular. We obtain a concrete formula for this spacing, namely,

$$\Delta H_x = \frac{\pi H_c}{JI(\lambda, \lambda_2)}, \quad (1.6)$$

where I is an integral expression [see Eq. (3.27)] depending on the parameters $\lambda = k_2/k_1$, $\lambda_2 = CJ^2/k_1$ (see also Table I). With the parameter values relevant to Fe₈, we obtain $I = 3.88$, giving $\Delta H_x = 0.409$ T. WS quote a period of 0.41 T. Compared to the model \mathcal{H}_0 , the period is increased by a factor $\pi(1 - \lambda)^{-1/2}/I = 1.552$. We relate I to a complete elliptic integral, and give various formulas for it in the Appendix.

In Sec. III B we turn to the jump instantons. We first formulate the equations for determining the endpoints of these instantons. In general these equations would have to be

solved numerically, but for the Fe_8 model, it turns out that an analytical solution can be found. With these endpoints in hand, we can find the complete instantons and their actions (this must still be done numerically). We use our computed actions for all the instantons to find the splitting as a function of magnetic field, and compare with the numerical diagonalization. This exercise is carried out for the value of λ_2 applicable to Fe_8 , as well as some others.

In Sec. IV we address the issue of the number of quenching points in light of general quantum mechanical theorems. It is not an accident that WS see an even number (four) of quenchings for $H_x > 0$. We will see that the general theorems constrain this number for any value of J , and then show how this same conclusion comes about from the instanton analysis.

We conclude the paper in Sec. V with a summary and discussion.

II. SU(2) INSTANTON FORMALISM REVISITED

The instanton method is an efficient way of calculating tunnel splittings, both for particles [25] and for spin [26]. It is based on evaluating the path integral for a certain propagator in the steepest-descent approximation, and is designed to be asymptotically correct in the semiclassical limit ($J \rightarrow \infty$ or $\hbar \rightarrow 0$). Instantons are classical paths that run between degenerate classical minima of the energy. By “classical” we mean that the path obeys the principle of least action, and, *a fortiori*, satisfies energy conservation. However, a path along which energy is conserved can not run between two minima and still have real coordinates and momenta. Hence, one must enlarge the notion of a classical path, and allow the coordinates and/or momenta to become complex. One is naturally led in this way to reexamine the least action principle. In the case of spin, there is yet another reason for this reexamination, as we shall see.

A. Spin coherent states and their parametrization

More specifically, let the degenerate classical energy minima be along the directions $\hat{\mathbf{n}}_i$ and $\hat{\mathbf{n}}_f$. We seek the propagator

$$K_{fi} = \langle \hat{\mathbf{n}}_f | \exp[-\mathcal{H}T] | \hat{\mathbf{n}}_i \rangle \quad (2.1)$$

in the limit $T \rightarrow \infty$. Here, $|\hat{\mathbf{n}}_{i,f}\rangle$ are spin coherent states (defined below). This propagator is given by the path integral

$$K_{fi} = \int \mathcal{D}[\hat{\mathbf{n}}(t)] e^{-S[\hat{\mathbf{n}}(t)]}, \quad (2.2)$$

where $\hat{\mathbf{n}}(0) = \hat{\mathbf{n}}_i$, $\hat{\mathbf{n}}(T) = \hat{\mathbf{n}}_f$, and S is the (Euclidean) action. When we evaluate this integral by steepest descents, least action paths emerge naturally.

We define the spin coherent state $|\hat{\mathbf{n}}\rangle$ as the state with maximal spin projection along the direction $\hat{\mathbf{n}}$. In other words, $\hat{\mathbf{n}}$ is an eigenstate of $\mathbf{J} \cdot \hat{\mathbf{n}}$ with eigenvalue J :

$$\mathbf{J} \cdot \hat{\mathbf{n}} |\hat{\mathbf{n}}\rangle = J |\hat{\mathbf{n}}\rangle. \quad (2.3)$$

The most common way of explicitly writing $|\hat{\mathbf{n}}\rangle$ and $S[\hat{\mathbf{n}}(\tau)]$ is in terms of the spherical polar coordinates θ and ϕ of the direction $\hat{\mathbf{n}}$. For formal purposes, another representation is more convenient. Let z be a complex number, related to (θ, ϕ) by the stereographic map

$$z = \tan \frac{\theta}{2} e^{i\phi}. \quad (2.4)$$

Then, up to normalization and phase, $|\hat{\mathbf{n}}\rangle$ is identical to the state [27]

$$|z\rangle = e^{zJ_-} |J, J\rangle. \quad (2.5)$$

The advantage of this representation is that matrix elements of various operators have nice analyticity properties. For example, for Hamiltonians polynomial in the components of \mathbf{J} ,

$$H(\bar{z}', z) = \frac{\langle z' | \mathcal{H} | z \rangle}{\langle z' | z \rangle} \quad (2.6)$$

is holomorphic in z and antiholomorphic in z' , where \bar{z} is the formal complex conjugate of z . In equations, this means that

$$\frac{\partial}{\partial \bar{z}} H(\bar{z}', z) = \frac{\partial}{\partial z'} H(\bar{z}', z) = 0. \quad (2.7)$$

Explicit model calculations, however, are often easier in θ and ϕ .

Since we will be considering paths on the complexified unit sphere, it is useful to understand what this means in terms of the two coordinate systems. Let u , v , and w be Cartesian coordinates in three-dimensional space. The real unit sphere is the surface specified by

$$u^2 + v^2 + w^2 = 1. \quad (2.8)$$

The complexified unit sphere is obtained by allowing u , v , and w to become complex. The real and imaginary parts of Eq. (2.8) provide two constraints among six variables (the real and imaginary parts of u , v , and w), leaving us with a four-dimensional manifold. We can also see this in the terms of polar and stereographic variables. Consider the former first. We relate them to Cartesian coordinates in the usual way

$$(u, v, w) = (\cos \theta, \sin \theta \cos \phi, \sin \theta \sin \phi). \quad (2.9)$$

Equation (2.8) is automatically satisfied. This continues to be true if we allow θ and ϕ to be complex. Once again, we conclude that four real quantities are required to specify a point on this manifold. Let us consider stereographic variables next. Since

$$z = \tan \frac{\theta}{2} e^{i\phi}, \quad \bar{z} = \tan \frac{\theta}{2} e^{-i\phi}, \quad (2.10)$$

we see that if θ and ϕ are complex, \bar{z} will not be the same as z^* , the true complex conjugate of z . To specify a point on the complex unit sphere, both z and \bar{z} are needed, i.e., four real parameters are needed. Conversely, a point with stereographic coordinates (\bar{z}, z) lies on the real unit sphere (which is a submanifold of the complex unit sphere) if z and \bar{z} are complex conjugates. Such points may be given by specifying z alone or \bar{z} alone. Thus, corresponding to the directions $\hat{\mathbf{n}}_i$ and $\hat{\mathbf{n}}_f$, which are real, we may speak of “the points” z_i and z_f , or “the points” \bar{z}_i and \bar{z}_f .

B. Action functional for spin

Let us now consider the action. To specify a path $\hat{\mathbf{n}}(t)$ on the unit sphere stereographically, one must give both $z(t)$ and $\bar{z}(t)$. The action (or more precisely, the Hamilton principal function) for a path obeying the boundary conditions

$$z(0) = z_i, \quad \bar{z}(T) = \bar{z}_f, \quad (2.11)$$

is given by [28, 29]

$$S(\bar{z}(t), z(t)) = S_K + S_D + S_B, \quad (2.12)$$

where

$$S_K = - \int_0^T \left[J \frac{\dot{\bar{z}}z - \bar{z}\dot{z}}{1 + \bar{z}z} \right] dt \quad (2.13)$$

$$S_D = \int_0^T H(\bar{z}, z) dt \quad (2.14)$$

$$S_B = -J \ln \left[\frac{(1 + \bar{z}(0)z_i)(1 + \bar{z}_f z(T))}{(1 + z_i^* z_i)(1 + z_f^* z_f)} \right]. \quad (2.15)$$

We refer to these terms as the kinetic, dynamical, and boundary terms, respectively. In S_B , $z_{i,f}^*$ denotes the *true* complex conjugate of $z_{i,f}$. This term depends explicitly on the boundary values of the path, and is needed to avoid the overdetermination problem [15, 16]. We state why this is so without proof. If we vary the path $\bar{z}(t)$, $z(t)$, *including the endpoints*, and require the resulting variation δS to vanish, we discover (i) the Euler-Lagrange (EL) equations

$$\dot{\bar{z}} = \frac{(1 + \bar{z}z)^2}{2J} \frac{\partial H}{\partial z}, \quad \dot{z} = -\frac{(1 + \bar{z}z)^2}{2J} \frac{\partial H}{\partial \bar{z}}, \quad (2.16)$$

and (ii) that δS has no terms proportional to $\delta\bar{z}(0)$ or $\delta z(T)$. This means that the action evaluated for the classical path $z_{\text{cl}}(t)$, $\bar{z}_{\text{cl}}(t)$ [which obeys Eqs. (2.11) and (2.16)] is not a function of $\bar{z}_i \equiv \bar{z}(0)$ and $z_f \equiv z(T)$:

$$\frac{\partial}{\partial \bar{z}_i} S^{\text{cl}} = \frac{\partial}{\partial z_f} S^{\text{cl}} = 0. \quad (2.17)$$

Equivalently, one can say that

$$S[\bar{z}_{\text{cl}}(t), z_{\text{cl}}(t)] = S^{\text{cl}}(\bar{z}_f, z_i, T), \quad (2.18)$$

where we show the variables on which S^{cl} depends explicitly. Third, one obtains the Hamilton-Jacobi equations

$$\frac{\partial S^{\text{cl}}}{\partial \bar{z}_f} = 2J \frac{z(T)}{1 + \bar{z}_f z(T)}, \quad \frac{\partial S^{\text{cl}}}{\partial z_i} = 2J \frac{\bar{z}(0)}{1 + \bar{z}(0)z_i}. \quad (2.19)$$

Lastly, the “energy” is conserved along the classical path:

$$\frac{d}{dt} H(\bar{z}_{\text{cl}}(t), z_{\text{cl}}(t)) = 0. \quad (2.20)$$

This follows from Eq. (2.16).

What would have happened if we had omitted the boundary term S_B in Eq. (2.12)? Since a general variation δS would include terms proportional to all four quantities δz_i , $\delta \bar{z}_i$, δz_f , and $\delta \bar{z}_f$, the classical path would have to be specified via four boundary conditions $(z_i, \bar{z}_i, z_f, \bar{z}_f)$, whereas the EL conditions would still form a system of differential equations of order 2. The system would be overdetermined with no solution in general. (The same

problem can be seen in spherical polar coordinates. One must give θ_i and ϕ_i to specify $\hat{\mathbf{n}}_i$, and θ_f and ϕ_f for $\hat{\mathbf{n}}_f$, i.e., four boundary conditions in all.) Second, even with only two boundary conditions $z(0) = z_i$, $\bar{z}(T) = \bar{z}_f$, for general z_i and \bar{z}_f there is no *real* solution to the EL equations. That is to say, $\bar{z}_{\text{cl}}(t)$ is not equal to the true complex conjugate of $z_{\text{cl}}(t)$. A solution will in general exist only if we allow $\bar{z}_{\text{cl}}(t)$ and $z_{\text{cl}}(t)$ to be independent complex functions. [In spherical polar coordinate language, we must allow both $\theta(t)$ and $\phi(t)$ to become complex.] We thus see that if we want to consider classical dynamics for spin from the viewpoint of a least action principle, we must allow the dynamics to live on the complexified unit sphere from the very outset.

We have couched the above discussion in language following Faddeev [15]. It is also useful to discuss Klauder's resolution of these issues [16]. On the face of it, his treatment is slightly different, but turns out to be equivalent to Faddeev's in actual applications. Klauder does not include an explicit boundary term in S , but argues that since the continuum path integral is a formal construct with meaning only as a limit of its discrete version, one may add a term to the integrand for S_K that is quadratic in the velocities $\dot{\theta}$ and $\dot{\phi}$, and which has an infinitesimal coefficient ϵ . The EL equations are then a fourth order system, and a classical solution always exists. However, it has the following structure. It evolves from (θ_i, ϕ_i) to a point $(\bar{\theta}_i, \bar{\phi}_i)$ (note the different use of the overbar) in a boundary layer of duration $O(\epsilon)$, evolves for a time $T - O(\epsilon)$ along a path $\bar{\theta}(t), \bar{\phi}(t)$ according to

$$iJ \sin \theta \frac{d\theta}{dt} = \frac{\partial H}{\partial \phi}, \quad iJ \sin \theta \frac{d\phi}{dt} = -\frac{\partial H}{\partial \theta}, \quad (2.21)$$

and then evolves from a point $(\bar{\theta}_f, \bar{\phi}_f)$ to (θ_f, ϕ_f) in another boundary layer of duration $O(\epsilon)$ near $t = T$. [Note that Eq. (2.21) is equivalent to Eq. (2.16).] The extra kinetic term in the action gives a non-zero contribution only from integration over the boundary layers, but this contribution is explicitly independent of ϵ as $\epsilon \rightarrow 0$. The net classical action is then given by

$$\begin{aligned} S^{\text{cl}} = & \int_0^T \left[iJ(1 - \cos \bar{\theta}) \dot{\bar{\phi}} + H(\bar{\theta}, \bar{\phi}) \right] dt \\ & + 2J \ln \left[\frac{\cos \frac{1}{2}\bar{\theta}_i \cos \frac{1}{2}\bar{\theta}_f}{\cos \frac{1}{2}\theta_i \cos \frac{1}{2}\theta_f} \right]. \end{aligned} \quad (2.22)$$

$$(2.23)$$

The last term is the boundary layer contribution, and is equivalent to the explicit term S_B

in Eq. (2.12) [30]. The boundary values $(\bar{\theta}_i, \bar{\phi}_i)$ and $(\bar{\theta}_f, \bar{\phi}_f)$ are constrained by

$$\tan \frac{1}{2}\bar{\theta}_i e^{i\bar{\phi}_i} = \tan \frac{1}{2}\theta_i e^{i\phi_i}, \quad (2.24)$$

$$\tan \frac{1}{2}\bar{\theta}_f e^{-i\bar{\phi}_f} = \tan \frac{1}{2}\theta_f e^{-i\phi_f}, \quad (2.25)$$

[note the similarity to $z(0) = z_i$, $\bar{z}(T) = \bar{z}_f$]. Once again a solution can in general be found only if $\bar{\theta}(t)$ and $\bar{\phi}(t)$ are complexified.

C. Structure of answer for Fe_8

Once the action functional is specified, the instanton recipe for calculating the tunnel splitting is as follows. Let there be a number of instantons, i.e., least action paths, labeled by k , and let the actions for these various paths be S_k^{cl} . The tunneling amplitude is given by

$$\Delta = \sum_k D_k e^{-S_k^{\text{cl}}}. \quad (2.26)$$

This can be understood as arising from the path integral (2.2) in the following way. In the integral, the dominant paths (in the sense of the method of steepest descents), are those for which the action is stationary. These are responsible for the exponential factor $\exp(-S_k^{\text{cl}})$. The prefactor D_k results from integrating out the Gaussian fluctuations around the k th instanton. The full expression for K_{fi} must include a sum over multi-instanton paths, and this leads to a result which is essentially exponential in Δ , in a way which is now well understood [25].

Up to now, all explicit instanton calculations of tunnel splittings of which we are aware have the property that the initial and final points of the instantons lie on the real unit sphere. In other words, $\bar{z}(0) = z_i^*$, $z(T) = \bar{z}_f^*$. In Klauder's language, $(\bar{\theta}_{i,f}, \bar{\phi}_{i,f}) = (\theta_{i,f}, \phi_{i,f})$, so there are no boundary layers in the path. (At intermediate times, of course, the path *is* complexified.) This is due to simplifying special features present in the models studied. As a result, there is no need to include the explicit boundary terms in S or S^{cl} , and the practice in all papers on spin instantons (including those written by one of us, AG), has been to forget about them altogether. In the present problem, however, we find that although instantons with end points on the real sphere still exist, one also has instantons for which this is not so. We refer to these as *boundary jump instantons* (BJI). It is essential to include the latter

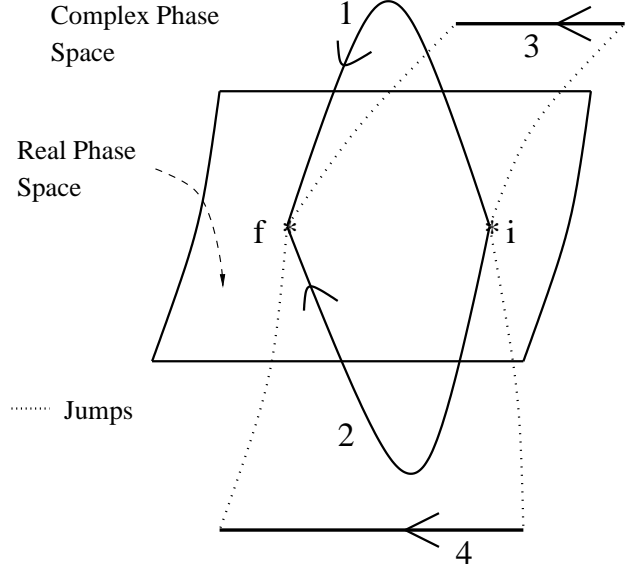


FIG. 2: Schematic of instanton paths in Fe₈. We show a portion of real phase space (the real unit sphere) as a two-dimensional surface, that is embedded in complex phase space. The latter is four-dimensional, but we can only represent it as three-dimensional in this perspective drawing. The initial and final points i and f lie in real phase space. Paths 1 and 2 start at these points, have no jumps, interfere with each other, and evolve smoothly as the C term in Eq. (1.4) is turned on. Except at the end points these paths lie in complex phase space. Paths 3 and 4 possess jumps at the end points, do not interfere, and are obtained only when $C \neq 0$. These paths lie entirely in complex phase space.

in order to understand why the number of diabolical points on the H_x axis is reduced from 10 to 4.

More specifically, we have four instantons, labeled 1, 2, 3 and 4 (see Fig. 2). The first two have no boundary jumps, and are the ones that interfere as in Ref. [4]. The third and fourth are boundary jump instantons. Hence,

$$\Delta = \sum_{k=1}^4 D_k e^{-S_k^{\text{cl}}}. \quad (2.27)$$

By proper choice of gauge, one can ensure that all D_i are real, S_3^{cl} and S_4^{cl} are real, and that $S_2^{\text{cl}} = (S_1^{\text{cl}})^*$, $D_2 = D_1$. More generally, the real parts of S_1^{cl} and S_2^{cl} must be equal to each other by symmetry, and the imaginary parts must be related by

$$S_2^{\text{cl}} - S_1^{\text{cl}} = 2iJ\Phi, \quad (2.28)$$

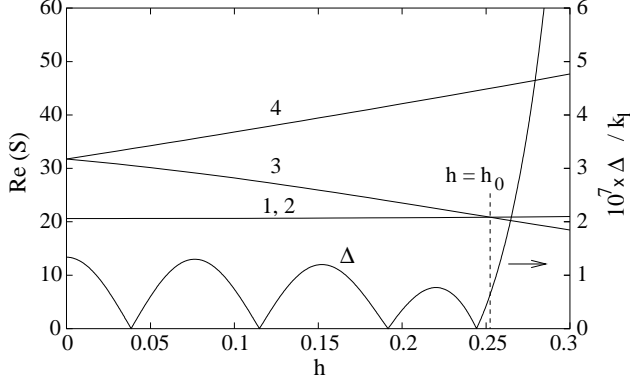


FIG. 3: Real parts of the actions versus the magnetic field for the four instantons in the Fe₈ problem. Also shown is the energy splitting between the ground level pair. For $h > h_0$, instanton number 3 is the dominant one, and since it has no interfering partner, the splitting rises with h instead of oscillating.

where Φ is half the area on the complexified unit sphere enclosed by the closed loop formed by taking instanton 1 from $\hat{\mathbf{n}}_i$ to $\hat{\mathbf{n}}_f$, and instanton 2 back to $\hat{\mathbf{n}}_i$. Therefore, we can write

$$\Delta = 2D_1 e^{-\text{Re} S_1^{\text{cl}}} \cos(J\Phi) + D_3 e^{-S_3^{\text{cl}}} + D_4 e^{-S_4^{\text{cl}}}. \quad (2.29)$$

All the quantities in this equation depend on the field H_x . We discover that $S_3^{\text{cl}} < S_4^{\text{cl}}$ for all fields. At low fields, $\text{Re} S_1^{\text{cl}} < S_3^{\text{cl}}$, while at high fields, the inequality is reversed. The two actions are equal at $h_0 = 0.25$ (see Fig. 3). The prefactors D_i set the dimensional scale for the tunneling, and are generally equal to classical small oscillation frequencies in order of magnitude. Thus we do not expect the D_i to be very different, and the relative importance of the different instantons is determined mainly by the S_i . Hence, ignoring a very small region in the immediate neighborhood of h_0 , we can write

$$\Delta \approx \begin{cases} 2D_1 e^{-\text{Re} S_1^{\text{cl}}} \cos(J\Phi), & h < h_0; \\ D_3 e^{-S_3^{\text{cl}}}, & h > h_0. \end{cases} \quad (2.30)$$

In particular, there will be no quenchings in Δ for $h_x > h_0$. For $h_x < h_0$, quenching will occur when $\Phi = (2n + 1)\pi/2J$, where n is an integer.

III. ANALYSIS FOR FE_8

A. The interfering instantons

We now turn to finding the instantons explicitly. For this purpose, it is better to use a coordinate system having z as the hard axis and x as the easy axis. Introducing spherical polar coordinates θ and ϕ in the standard way, the energy (expectation value of the Hamiltonian) in this frame is given by

$$\begin{aligned} E(\theta, \phi) = & \lambda \sin^2 \theta \sin^2 \phi + \cos^2 \theta - 2h \cos \theta \\ & - 2\lambda_2 (\cos^4 \theta + \sin^4 \theta \sin^4 \phi - 6 \sin^2 \theta \cos^2 \theta \sin^2 \phi). \end{aligned} \quad (3.1)$$

The first step is to find the minimum of this energy. Setting $\partial E / \partial \theta$ and $\partial E / \partial \phi$ to zero, we obtain

$$\cos \phi \sin \phi [24\lambda_2 \sin^2 \theta \cos^2 \theta - 8\lambda_2 \sin^4 \theta \sin^2 \phi + 2\lambda \sin^2 \theta] = 0 \quad (3.2)$$

and

$$\begin{aligned} \sin \theta [2\lambda \cos \theta \sin^2 \phi - 2 \cos \theta + 2h + 8\lambda_2 \cos^3 \theta \\ - 8\lambda_2 (\sin^2 \theta \sin^2 \phi + 6 \sin^2 \theta - 1) \cos \theta \sin^2 \phi] = 0. \end{aligned} \quad (3.3)$$

When these conditions are examined carefully, it is found that the minima occur when $\phi = 0, \pi$ and the expression in the square brackets in the second equation is zero, i.e., at $\phi = 0, \pi$ and at $\theta = \theta_0$ where θ_0 obeys

$$\cos \theta_0 - h - 4\lambda_2 \cos^3 \theta_0 = 0, \quad (3.4)$$

The minimum energy is

$$E_{\min} = \cos^2 \theta_0 - 2h \cos \theta_0 - 2\lambda_2 \cos^4 \theta_0, \quad (3.5)$$

Since $\zeta = 4\lambda_2 h^2 \ll 1$ for all h , one can solve Eq. (3.4) perturbatively to get $\cos \theta_0 = h + 4\lambda_2 h^3$ to first order in ζ . In the same approximation, $E_{\min} = -h^2 - 2\lambda_2 h^4$.

Next, let us find the instantons. The trajectory, i.e., the path in phase space without regard to the time dependence, can be found by exploiting energy conservation. With the abbreviations

$$u = \cos \theta, \quad s = \sin \phi, \quad (3.6)$$

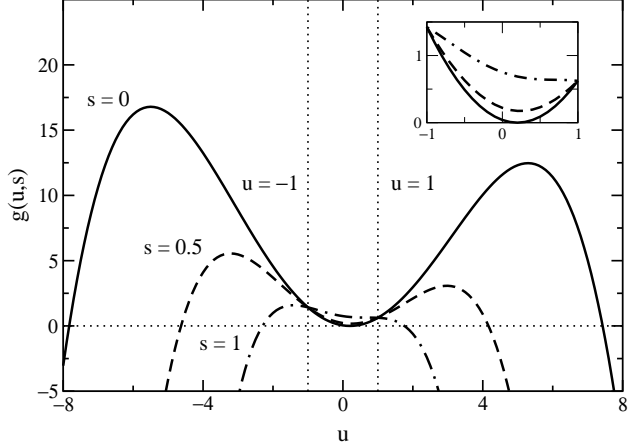


FIG. 4: Plot of $g(u, s)$ versus u for various s . The points to note are that (i) except when $s = 0$, g has no zeros in the interval $[-1, 1]$, (ii) g always has two zeros outside this interval. For $s = 0$, g has a double zero at some $u \in [-1, 1]$. The inset shows an enlarged view of g in the same interval.

the condition $E(\theta, \phi) = E_{\min}$ can be written as

$$g(u, s) = -\frac{1}{2}Z(s)u^4 + R(s)u^2 - 2hu + W(s) = 0, \quad (3.7)$$

where

$$Z(s) = 4\lambda_2(1 + 6s^2 + s^4), \quad (3.8)$$

$$R(s) = 1 - \lambda s^2 + 12\lambda_2 s^2 + 4\lambda_2 s^4, \quad (3.9)$$

$$W(s) = g_0 + h^2 + \lambda s^2 - 2\lambda_2 s^4, \quad (3.10)$$

with

$$g_0 = -(\lambda + h^2) - E_{\min} \approx 2\lambda_2 h^4 + O(h^6). \quad (3.11)$$

Equation (3.7) may be solved as a quartic equation for $u(s)$. Let us first consider only real values of ϕ , and thus of s . It is useful to sketch $g(u, s)$ as a function of u for real u , and fixed s , remembering that $|s| \leq 1$ (see Fig. 4). Consider first the interval $-1 \leq u \leq 1$, corresponding to points (θ, ϕ) on the real unit sphere. Since $g = E - E_{\min}$, it must be nonnegative in this interval. In fact, for $s \neq 0$, it must be *strictly* positive, and for $s = 0$, it vanishes only at one point, $u = \cos \theta_0$, where it has a double zero. Secondly, $g \rightarrow -\infty$ as $u \rightarrow \pm\infty$. It follows that for $|s| \leq 1$, $g(u, s)$ always has exactly two real roots $u(s)$, with $|u(s)| > 1$. These roots can not be the instantons that tend to the true energy minima as $t \rightarrow \pm\infty$. Those roots are the complex conjugate pair with both real and imaginary parts.

For the complex roots let $u = A + iB$ with A and B being real. From the imaginary part of Eq. (3.7) we obtain the equation

$$-2Z(A^3B - AB^3) + 2RAB - 2hB = 0, \quad (3.12)$$

while the real part yields

$$-\frac{1}{2}Z(A^4 - 6A^2B^2 + B^4) + R(A^2 - B^2) - 2hA + W = 0. \quad (3.13)$$

Since we are not interested in solutions with either $A = 0$ or $B = 0$, Eq. (3.12) implies that

$$B^2 = A^2 - (R/Z) + (h/AZ). \quad (3.14)$$

Substituting this into Eq. (3.13), we obtain an equation for A alone:

$$4Z^2A^6 - 4RZA^4 + (R^2 + 2WZ)A^2 - h^2 = 0, \quad (3.15)$$

which is a cubic in A^2 .

When $\lambda_2 = 0$, $Z(s) = 0$, and Eq. (3.15) has the solution $A = h/R = h/(1 - \lambda \sin^2 \phi)$. We seek that solution of the cubic which tends to this solution as $\lambda_2 \rightarrow 0$. We can obtain this approximately if we assume that $A = O(h)$. The terms $Z A^4$ and $Z^2 A^6$ are of order ζ and ζ^2 respectively, relative to the remaining two terms in Eq. (3.15). If we drop the former two terms, the remaining equation is trivially solved to obtain

$$A = \frac{h}{(R^2 + 2WZ)^{1/2}}, \quad (3.16)$$

which is in fact of $O(h)$. Thus, our assumption is self-consistently verified, and the solution has the correct behavior as $\lambda_2 \rightarrow 0$.

Next, we note that

$$R^2 + 2WZ = P'_0 + P'_2 \sin^2 \phi + P'_4 \sin^4 \phi, \quad (3.17)$$

where we have unabbreviated s , and

$$P'_0 = 1 + 8\lambda_2(h^2 + g_0) \approx (1 + \zeta)^2, \quad (3.18)$$

$$P'_2 = -2\lambda + 24\lambda_2 + 8\lambda\lambda_2 + 12\zeta + 48\lambda_2g_0, \quad (3.19)$$

$$\approx -2\lambda + 24\lambda_2 + 8\lambda_2\lambda + 12\zeta + 6\zeta^2, \quad (3.20)$$

$$P'_4 = \lambda^2 + 8\lambda_2 + 24\lambda\lambda_2 + 128\lambda_2^2 + 2\zeta + 8\lambda_2g_0. \quad (3.21)$$

$$\approx \lambda^2 + 8\lambda_2 + 24\lambda\lambda_2 + 128\lambda_2^2 + 2\zeta + \zeta^2. \quad (3.22)$$

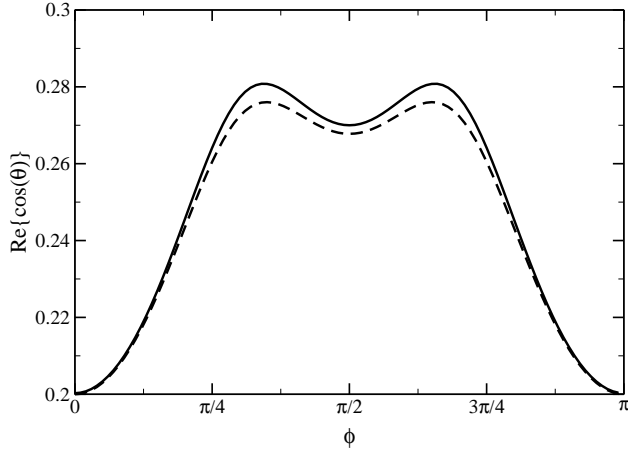


FIG. 5: Plot of $\text{Re} \cos \theta$ versus ϕ for $h = 0.2$ and the Fe_8 parameters. The solid line is from exact numerical solution of $g(u, s) = 0$, and the dashed line is the approximation (3.23).

All three coefficients depend on h only through the combination $\zeta = 4\lambda_2 h^2$, which is very small. If we neglect this weak dependence, we get $A \approx A_0$, where

$$A_0 = \frac{h}{(1 + P_2 \sin^2 \phi + P_4 \sin^4 \phi)^{1/2}}, \quad (3.23)$$

with

$$P_2 = -2\lambda + 24\lambda_2 + 8\lambda_2\lambda, \quad (3.24)$$

$$P_4 = \lambda^2 + 8\lambda_2 + 24\lambda\lambda_2 + 128\lambda_2^2. \quad (3.25)$$

For completeness, we mention that it is possible to systematically obtain corrections to A in powers of ζ , in the form $A_0 + \zeta A_1 + \dots$. We do not carry out this exercise here. To see how good Eq. (3.23) is, we plot the real part of $\cos \theta$ in Fig. 5. The dashed line is our approximation, and the solid line is obtained by numerically solving $E - E_{\min} = 0$ with the numerically exact value of E_{\min} . In this plot, h is taken to be 0.2. It can be seen that the two curves agree very well.

With Eq. (3.23), we can now calculate the imaginary part of the tunneling action, and the Berry phase $2J\Phi$ of Eq. (2.28). We have

$$\begin{aligned} \Phi &= \int_0^\pi (1 - A) d\phi \\ &\approx [\pi - hI(\lambda, \lambda_2)], \end{aligned} \quad (3.26)$$

where

$$I(\lambda, \lambda_2) = \int_0^\pi \frac{1}{(1 + P_2 \sin^2 \phi + P_4 \sin^4 \phi)^{1/2}} d\phi. \quad (3.27)$$

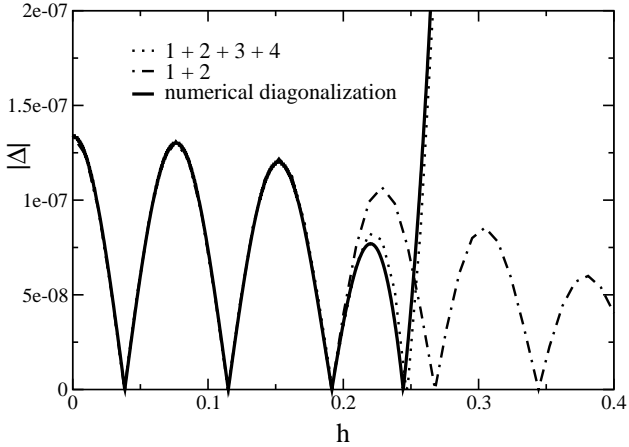


FIG. 6: Tunnel splitting (in Kelvin) between ground level pair for the model (1.4), as computed by numerical diagonalization of the Hamiltonian (solid line), in the instanton approximation keeping only instantons 1 and 2 (dot-dashed line), and in the instanton approximation with all four instantons (dotted line). We take all prefactors D_i to be equal and independent of h , and adjust the common value so as to obtain the correct answer for Δ at $h = 0$.

Various formulas for this integral are given in the Appendix.

The quenching condition $J\Phi = (n + \frac{1}{2})\pi$ gives the diabolical points as

$$h = \frac{(2J - 2n - 1)\pi}{2JI}, \quad (3.28)$$

where n is an integer. For Fe_8 , $I = 3.88$ as stated in Sec. I. The observed diabolical points agree extremely well with Eq. (3.28). In particular, Eq. (3.28) gives the period $\Delta H = 0.409$ T. The experimental period is 0.41 T.

We can now see why the diabolical points in Fe_8 are so regularly spaced. This is because A is linear in h to very good approximation. Corrections to Eq. (3.28) can be found by including the correction A_1 . This may be important for the new system in which Δ oscillations are indicated [3].

At this point, we could use Eq. (3.14) and our approximation $A \approx A_0 + \zeta A_1$ to find $B(\phi)$, and thus $\text{Re } S_1^{\text{cl}}$. Since the resulting analysis is not completely analytical, we forgo it, and instead, solve for the instanton trajectory $\cos \theta(\phi)$ and evaluate the integral for the action S_1 numerically. The instantons are shown in Fig. 3 of Ref. 17, and the resulting approximation for Δ is shown in Fig. 6. We do not know the prefactor D_1 , but it is clear that it is a very good approximation to take it to be independent of H . It is also clear, however, that the

interfering instantons can not account for the behavior of Δ for $h > h_0$. For that, we must turn to the boundary jump instantons.

B. The Boundary-Jump (Noninterfering) Instantons

The instantons we have found above have the properties (a) $\bar{z}_i = z_i^*$, $z_f = (\bar{z}_f)^*$, and (b) $H(\bar{z}_i, z_i) = H(\bar{z}_f, z_f) = E_{\min}$. As discussed earlier, however, only z_i and \bar{z}_f are fixed, and one need not have $\bar{z}_i = z_i^*$ or $z_f = (\bar{z}_f)^*$. Let us suppose that we start the evolution of the Euler-Lagrange equations (2.16) from a point (\bar{z}_i, z_i) , with $\bar{z}_i \neq z_i^*$. Whatever this point is, it follows from Eq. (2.20) that the energy $H(\bar{z}, z)$ must be conserved along the trajectory, and must be equal to $E = H(\bar{z}_i, z_i)$. Conversely, if the value of E is known, we can determine the possible values of \bar{z}_i by solving the equation $H(\bar{z}, z_i) = E$. For the non-boundary-jump instantons, $E = E_{\min}$. The issue is what value of E we should use for the instantons with jumps.

The answer is that we must take $E = E_{\min}$ for the jump instantons too. The easiest way to see this is in Klauder's formalism. His extra kinetic term is

$$S'_K = 4\epsilon \int_0^T \frac{1}{(1 + \bar{z}z)^2} \dot{z} \dot{z} dt. \quad (3.29)$$

It is easy to write down the new Euler-Lagrange equations, and see that energy is once again conserved. Suppose there is a boundary layer in the solution of the EL equations around $t = t_0$. Since, as $\epsilon \rightarrow 0$, the boundary layer turns into a jump, and the extra kinetic energy vanishes for times $t = t_0+$ or t_0- , the energy before and after the jump must be the same.

The problem of finding the boundary-jump instantons (indeed, all instantons) can therefore be posed as follows. Let the “classical” Hamiltonian $H(\bar{z}', z)$ have minima at (z_i^*, z_i) , (z_f^*, z_f) , and let its value at these points be E_{\min} . Then we find all possible values of \bar{z}_i by solving the equation

$$H(\bar{z}, z_i) = E_{\min}. \quad (3.30)$$

This equation has a double root at $\bar{z} = z_i^*$, since

$$\frac{\partial}{\partial \bar{z}} H(\bar{z}, z) \bigg|_{z_i^*, z_i} = \frac{\partial}{\partial z} H(\bar{z}, z) \bigg|_{z_i^*, z_i} = 0. \quad (3.31)$$

It may, however, have additional roots at $\bar{z}_i \neq z_i^*$. These will be the initial points of boundary jump instantons. (Final points z_f are obtained in exactly the same way by solving

$H(\bar{z}_f, z) = E_{\min}.$) We then find all possible instantons $\bar{z}(z)$ as solutions to the equation $H(\bar{z}, z) = E_{\min}$, and identify which solution connects on to which end point. The time dependence is not needed to compute the action. For, the kinetic term can be written as

$$S_K = -J \int_{z_i}^{z_f} \frac{1}{1 + z\bar{z}(z)} \left[z \frac{d\bar{z}}{dz} - \bar{z}(z) \right] dz \quad (3.32)$$

$$= iJ \int_{\bar{\phi}_i}^{\bar{\phi}_f} (1 - \cos \bar{\theta}) d\bar{\phi}, \quad (3.33)$$

the dynamical term equals

$$S_D = E_{\min} T \quad (3.34)$$

for all instantons, and the boundary term S_B depends only on the boundary values, vanishing for the instantons without jumps.

For our Fe_8 Hamiltonian, the argument following Eqs. (3.7)–(3.11) shows that we have already found all the instantons without jumps. To find the jump instantons, let us first note that $(\theta_i = \theta_0, \phi_i = 0)$, and $(\theta_f = \theta_0, \phi_f = \pi)$. The constraints on z_i and \bar{z}_f therefore reduce to

$$\tan \frac{1}{2}\bar{\theta}_i e^{i\bar{\phi}_i} = \tan \frac{1}{2}\theta_0, \quad (3.35)$$

$$\tan \frac{1}{2}\bar{\theta}_f e^{-i\bar{\phi}_f} = -\tan \frac{1}{2}\theta_0. \quad (3.36)$$

Because of the symmetry of the problem, solving either of these equations will be enough for deducing the solution of the other. Let us solve for the initial values. First, Eq. (3.35) can be solved for $\sin \bar{\phi}_i$ to yield

$$\sin^2 \bar{\phi}_i = - \left(\frac{\cos \bar{\theta}_i - \cos \theta_0}{\sin \bar{\theta}_i \sin \theta_0} \right)^2. \quad (3.37)$$

Substituting this formula and Eqs. (3.1) and (3.5) into the energy conservation condition $E(\bar{\theta}_i, \bar{\phi}_i) = E_{\min}$ yields

$$\begin{aligned} 0 = & -\lambda \left(\frac{\cos \bar{\theta}_i - \cos \theta_0}{\sin \theta_0} \right)^2 + (\cos^2 \bar{\theta}_i - \cos^2 \theta_0) - 2h(\cos \bar{\theta}_i - \cos \theta_0) \\ & - 2\lambda_2 \left[\cos \bar{\theta}_i^4 + \left(\frac{\cos \bar{\theta}_i - \cos \theta_0}{\sin \theta_0} \right)^4 + 6 \cos^2 \bar{\theta}_i \left(\frac{\cos \bar{\theta}_i - \cos \theta_0}{\sin \theta_0} \right)^2 - \cos^4 \theta_0 \right]. \end{aligned} \quad (3.38)$$

We now eliminate h from this equation using Eq. (3.4). After some straightforward but lengthy algebra, we obtain

$$(\cos \bar{\theta}_i - \cos \theta_0)^2 \left[1 - \frac{\lambda}{\sin^2 \theta_0} - 2\lambda_2 b(\theta_i, \theta_0) \right] = 0, \quad (3.39)$$

where

$$b(\theta_i, \theta_0) = \cos^2 \bar{\theta}_i + 2 \cos \bar{\theta}_i \cos \theta_0 + 3 \cos^2 \theta_0 + \frac{(\cos \bar{\theta}_i - \cos \theta_0)^2}{\sin^4 \theta_0} + 6 \frac{\cos^2 \bar{\theta}_i}{\sin^2 \theta_0}. \quad (3.40)$$

There are four solutions to Eq. (3.39). The first two are the non-jump solutions, $\cos \bar{\theta}_i = \cos \theta_0$. The other two, which are the jump solutions obey

$$1 - \frac{\lambda}{\sin^2 \theta_0} - 2\lambda_2 b(\theta_i, \theta_0) = 0. \quad (3.41)$$

This is a quadratic equation for $\cos \theta_i$. For $h < 1$ and small λ_2 it is easy to check that in both solutions, $\cos \bar{\theta}_i$ is real and greater than unity. Hence, we may write $\bar{\theta}_i = i\nu_0$, where ν_0 is real. Equation (3.35) then shows that $\bar{\phi}_i$ may be taken in the form $\frac{1}{2}\pi - i\mu_0$, with μ_0 real.

It is easy to see that Eqs. (3.38)–(3.41) continue to hold if θ_i is replaced by θ_f . Thus the possible values for θ_f are the same as those for θ_i . Numbering the instantons in question 3 and 4, we have either $\theta_f^{(3)} = \theta_i^{(4)}$, or $\theta_f^{(3)} = \theta_i^{(3)}$. Symmetry suggests (and explicit numerics verifies) that the latter possibility is the correct one. If we then divide Eq. (3.36) by Eq. (3.35), we see that $\phi_f = \pi - \phi_i$. Thus, the end points are related by the symmetry of reflection in the hard-medium plane, i.e., $(J_e, J_m, J_h) \rightarrow (-J_e, J_m, J_h)$, where the suffixes e , m , and h stand for easy, medium, and hard.

If we parametrize $\bar{\theta}(t)$ and $\bar{\phi}(t)$ as $i\nu(t)$ and $(\pi/2) + i\mu(t)$, then it is easy to verify from the equations of motion that $\mu(t)$ and $\nu(t)$ stay real at all t . With this parametrization, the kinetic term in the action for instantons 3 and 4 may be written as

$$S_K = J \int_{-\mu_0}^{\mu_0} [\cosh \nu(\mu) - 1] d\mu, \quad (3.42)$$

which is real. The boundary contribution is

$$S_B = 4J \ln \left[\frac{\cosh(\nu_0/2)}{\cos(\theta_0/2)} \right], \quad (3.43)$$

which is also real. Hence the total action for the jump instantons is real.

The explicit calculation of the actions must be done numerically. We solve for the trajectories in the form $\nu(\mu)$ using energy conservation, making sure that the end points are correct. All these calculations are done as a function of h . The results for S_k^{cl} have already been shown in Fig. 3. We can also calculate the splitting using Eq. (2.30), taking $D_3 = D_1$, and fixing D_1 as before. The result is shown in Fig. 6. As can be seen, the agreement with

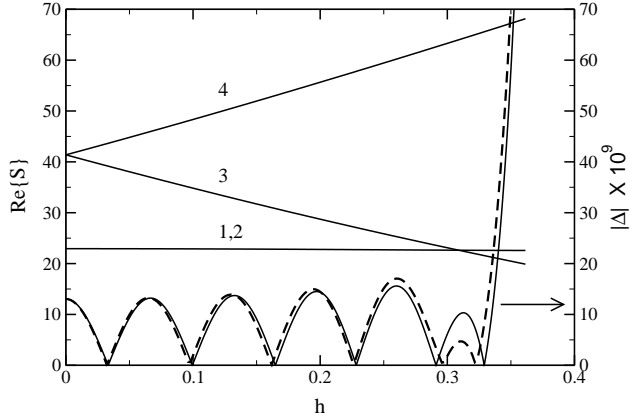


FIG. 7: Same as Fig. 3, but for $C = 1.2 \times 10^{-5}$ K. In addition to the splitting Δ obtained by numerical diagonalization of the Hamiltonian matrix (solid line), we show the answer given by Eq. (2.29) (dashed line) with all prefactors chosen to be equal, and adjusted so as to agree with the numerically computed splitting at $h = 0$.

the exact diagonalization is rather good. The t -dependence of \mathbf{J} for instanton number 3 is shown in Fig. 2 of Ref. 17. The jumps are evident in this figure.

We have also carried out this exercise for $C = 1.2 \times 10^{-5}$ K. The results are shown in Fig. 7. The general quality of the instanton approach is again very good, but it is weaker near the point where $S_3^{\text{cl}} = \text{Re } S_1^{\text{cl}}$. The obvious reason is that we have not considered the variation with h of the prefactors, especially D_3 . If we decrease C by yet another factor of 4, Eq. (2.29) with a single, h -independent prefactor $D_1 = D_3$, gives six quenching points instead of eight as found numerically. These considerations show that the prefactors are not always unimportant; at present, however, we only know how to find them for the non-jump instantons [31], and their calculation for jump instantons is an open problem.

C. Is the fourth-order anisotropy a singular perturbation?

In the previous subsection we showed that jump instantons exist for any $\lambda_2 \neq 0$. The character of the least action or “classical” paths for the problem is qualitatively altered by the fourth order term in Eq. (1.4), and from the point of view of the semiclassical analysis, therefore, this term is a singular perturbation. Viewed as a quantum mechanical operator, however, it is clear that the term is nonsingular; an infinitesimal nonzero value of λ_2 can not change the qualitative nature of the energy spectrum. We therefore refer to the perturbation

as quasisingular.

It follows from this consideration that a formal analysis of the instanton approach in the $\lambda_2 \rightarrow 0$ limit will necessarily be rather delicate. We describe briefly some analysis that shows why this is so.

We focus on jump instanton number 3, as this is clearly the most important new contributor. For this instanton, we discover that

$$\mu_0 = \frac{1}{2} \ln \left(\frac{1+u_0}{1-u_0} \right) + O(\lambda_2)^{1/2}, \quad (3.44)$$

where $u_0 = \cos \theta_0$, which is given by Eq. (3.4). Secondly, to leading order in λ_2 ,

$$\cosh \nu = \frac{1}{\sqrt{2\lambda_2}} \left[\frac{1 - \lambda \cosh^2 \mu}{1 + 6 \cosh^2 \mu + \cosh^4 \mu} \right]^{1/2}. \quad (3.45)$$

Because of this $\lambda_2^{-1/2}$ dependence, the leading term in the action S_3^{cl} is also of order $\lambda_2^{-1/2}$. The next term is proportional to $J \ln \lambda_2$. While the latter is well behaved as $\lambda_2 \rightarrow 0$ (remember that S^{cl} must be exponentiated), the former is not. It is clear that there must be a cancellation due to a corresponding term in D_3 , but we have not attempted to find this. This analysis shows that the success of our assumptions about the scale and h -independence of the prefactors is somewhat fortuitous. However, this assumption is the natural one in a semiclassical approach.

IV. NUMBER OF QUENCHING POINTS

A. Berry phase argument

That the tunnel splitting between two states vanishes is just another way of saying that the states are degenerate. The magnetic fields at which such degeneracy occurs form a set of isolated points in the magnetic field space (H_x , H_y , H_z), that are said to be *diabolical*, following Berry and Wilkinson [32]. Since these points are singularities of the energy surface, there are strong constraints on their creation or destruction as a perturbation is continuously varied. The number of diabolical points on the $H_x = 0$ axis is known when $C = 0$; it is interesting to inquire how many may remain when C is turned on, and to pursue this inquiry for general J , not just $J = 10$, and also consider fields in the xz plane [33]. (Simple physical arguments show that there can be no degeneracy if there is a component of the field along $\hat{\mathbf{y}}$.)

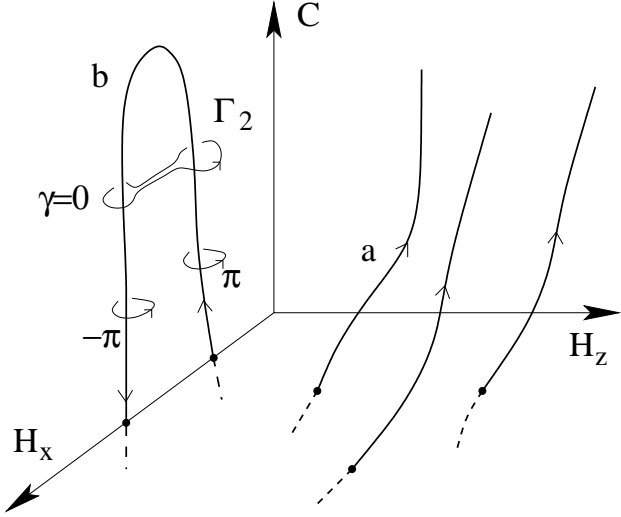


FIG. 8: Trajectories of diabolical points under the influence of the fourth order perturbation $-C(J_+^4 + J_-^4)$ in Eq. (1.4). The numbers 0 and $\pm\pi$ are the Berry phases associated with the adjacent contours.

Let us first take $C = 0$. With $H_y \neq 0$, in the standard representation of the spin operators, the matrix of the Hamiltonian is real. By a general theorem [34], the codimension of a degenerate eigenvalue of a real Hermitean matrix is 2. Hence, the degeneracies must occur at isolated points in the H_x - H_z plane. When C is turned on, each one of these points must turn into a line in the three-dimensional (H_x, H_z, C) space. The only two kinds of behaviors that are permitted by the theorem are shown in Fig. 8. The first kind, marked ‘a’, is a diabolical point that continues on for ever. The second kind, marked ‘b’, shows that two distinct diabolical points in the $C = 0$ plane actually lie on the same diabolical line in the three-dimensional space. (Of course, a similar turnaround could connect the two lines marked a and b for some $C < 0$, or the line b could form a closed loop.)

Is it possible for one of the diabolical lines to terminate abruptly? An argument based on Berry’s phase [35] shows that the answer is no. Let \mathbf{H} now denote the two-dimensional vector (H_x, H_z) . Let two states $|\psi_1(C, \mathbf{H})\rangle$ and $|\psi_2(C, \mathbf{H})\rangle$ be degenerate at $\mathbf{H} = \mathbf{H}_0 \equiv (H_{x0}, H_{z0})$ for some value of C , and let Γ be a small closed contour in the H_x - H_z plane around the point \mathbf{H}_0 . Berry’s phase, given by

$$\gamma(\Gamma) = i \oint_{\Gamma} \langle \psi_1(C, \mathbf{H}) | \nabla_{\mathbf{H}} \psi_1(C, \mathbf{H}) \rangle, \quad (4.1)$$

equals $\pm\pi$ if Γ encloses a diabolical point. Otherwise, $\gamma = 0$. Since a small change in C or \mathbf{H}

gives rise to a nonsingular perturbation of the Hamiltonian, the state $\psi_1(C, \mathbf{H})$ is a smooth function of C and \mathbf{H} . Hence the integrand of Eq. (4.1) can not change discontinuously under a continuous change of C , and the integral must not change at all. Thus the contour Γ must continue to encircle a degeneracy at small non zero C if it did so at $C = 0$.

From this point of view, the behavior ‘b’ in Fig. 8 can arise only if γ has opposite values for the two diabolical points at $C = 0$. The Berry phase for a contour Γ_2 encircling both points is then 0, and it is possible that for larger values of C , the contour can be shrunk to a point without running into any singularity. Plainly, this can happen only if the two points annihilate each other at some C . We can think of simply slipping the contour Γ_2 off the diabolical line by lifting it above the hairpin bend in the figure.

It follows that diabolical points can only disappear in pairs. For the problem of interest to us, degeneracy between ground levels, the points are constrained to occur when $H_z = 0$ (consider the behavior of the Hamiltonian under a 180° rotation about $\hat{\mathbf{x}}$). Our analysis shows that with increasing C , the points at larger H_x are removed first. Since the quenching points for any value of J are located as given by Eq. (1.2) when $C = 0$, it follows that when $C \neq 0$, the number N_q of such points for $H_x > 0$ must depend on J as follows:

$$\begin{aligned}
 2J & N_q \\
 4n & \text{even} \\
 4n+1 & \text{even} \\
 4n+2 & \text{odd} \\
 4n+3 & \text{odd}
 \end{aligned} \tag{4.2}$$

The same number must occur for $H_x < 0$. And, if J is half-integral, there must be a quenching point at $H_x = 0$, consistent with Kramer’s theorem. For Fe_8 , $J = 10$ and $N_q = 4$, which is consistent with these general rules.

B. Instanton based argument

Let us now see how our instanton analysis yields the same conclusion. For this, let us ignore the fourth instanton, and write the amplitudes due to the remaining instantons as [36]

$$\Delta_{1+2} = D_1(e^{-S_1^{\text{cl}}} + e^{-S_2^{\text{cl}}}), \tag{4.3}$$

$$\Delta_3 = D_3 e^{-S_3^{\text{cl}}}. \quad (4.4)$$

The keystone of our argument is the relative sign of the two amplitudes Δ_{1+2} and Δ_3 , in particular, the fact that

$$\text{sgn}(\Delta_{1+2}) = \text{sgn}(\Delta_3) \text{ for large } h. \quad (4.5)$$

By “large h ”, we mean that h is just less than the field strength at which the two classical minima in the energy merge into one. We shall not try and prove Eq. (4.5) with mathematical rigor [37]. Rather, we argue that it is physically plausible, for at such large fields, only spin orientations in a very small angular range are important, and one can use the Holstein-Primakoff, Villain, or any of a number of similar mappings to approximate the spin operators in terms of Q and P , position and momentum operators for a particle in one dimension. The problem is thereby mapped on to a particle in a double well in one dimension, for which the splitting never vanishes. Were Eq. (4.5) not true, it is conceivable that we could make $\Delta_{1+2} + \Delta_3$ vanish by varying the relative value of C and $(k_1 - k_2)$.

The second point is that the sign of Δ_3 should not change with h , since instanton 3 acts alone and has a real action. We may therefore take $D_3 > 0$, so that $\Delta_3 > 0$ for all h .

The third and last point is that the sign of Δ_{1+2} at $h = 0$ is now fixed by the requirement that this amplitude vanish the correct number of times between 0 and large h . Readers can verify that a correct assignment is obtained by taking

$$\Delta_1 = 2D_1 e^{-\text{Re}S_1^{\text{cl}}} \cos(J\pi), \quad (h = 0), \quad (4.6)$$

with $D_1 > 0$.

The rest of the argument is simple. Continuing to ignore the fourth instanton, the condition $\Delta = 0$ can be rewritten as

$$\Delta_3 = -\Delta_{1+2}. \quad (4.7)$$

We now simply sketch both sides of Eq. (4.7) as a function of h , keeping in mind the three points made above. This is done in Fig. 9 for all four classes of J listed in Eq. (4.2). In each case, it is obvious that the number of zeros, N_q , is exactly as given in this equation. In particular, it is obvious that N_q can change only in steps of two if the curve for Δ_3 is raised or lowered [38].

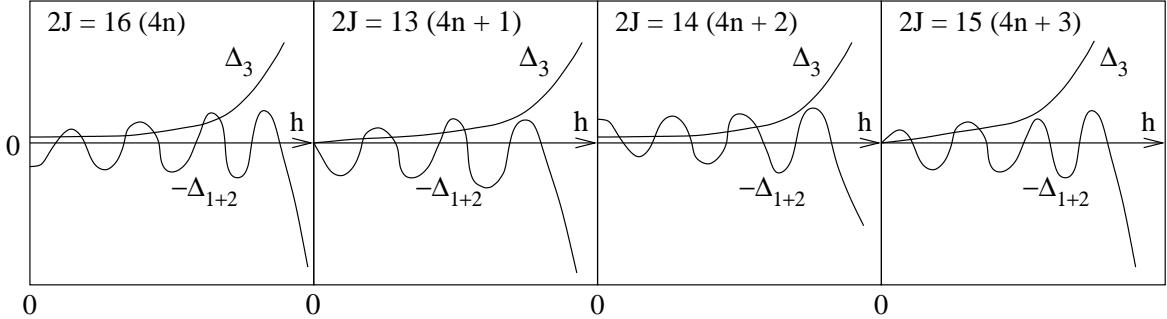


FIG. 9: Sketch of $-\Delta_{1+2}$ and Δ_3 versus h for all four classes of J listed in Eq. (4.2). The quenching points are given by the intersections of these two curves. The key points to note in each case are the number of zeros of Δ_{1+2} and the number of quenching points.

V. CONCLUSION

We have shown that the instanton formalism for spin coherent state path integrals requires the inclusion of instantons with discontinuities at the end points as a general matter. Such instantons are essential to understanding the magnetic field dependence of the tunnel splitting in Fe_8 . We have shown that with certain plausible assumptions about the prefactors, the instanton approximation can be quantitatively accurate. However, proper calculation of tunneling prefactors for the instantons with jumps remains an open problem.

Since jump instantons arise as a result of overspecification of boundary conditions, and since this overspecification is a necessary consequence of the coherent state formulation, it is clear that similar instantons will in general be present in *all* path integrals based on coherent states. For spin, such path integrals are unavoidable if one wishes to treat all spin orientations on an equal footing, and they are the only way of passing to the classical limit of the dynamics. This is not so for massive particles. Nevertheless, there may well be some problems that are better formulated in terms of coherent states, and then one will have to be alert to the presence of jump instantons. An explicit instance where this is so remains to be found.

Acknowledgments

One of us (AG) would like to acknowledge insightful discussions with Michael Stone on spin coherent state path integrals, and Jacques Villain on diabolical points.

*

APPENDIX A: THE OSCILLATION PERIOD INTEGRAL

In this appendix, we provide some formulas for the oscillation period integral (3.27), which we reproduce here for convenience:

$$I(\lambda, \lambda_2) = \int_0^\pi \frac{1}{(1 + P_2 \sin^2 \phi + P_4 \sin^4 \phi)^{1/2}} d\phi. \quad (\text{A1})$$

For Fe_8 , the constants P_2 and P_4 equal -1.200 and 0.7576 respectively. The integrand is real with these numbers.

Let w be a complex number such that

$$w + w^* = -P_2, \quad ww^* = P_4. \quad (\text{A2})$$

Then, using formula 2.616.1 of Ref. [39], we have

$$I = 2 \int_0^\pi \frac{d\phi}{[(1 - w \sin^2 \phi)(1 - w^* \sin^2 \phi)]^{1/2}} = \frac{2}{\sqrt{1-w}} K \left(\sqrt{\frac{w^* - w}{1 - w}} \right), \quad (\text{A3})$$

where $K(k)$ is the complete elliptic integral of the first kind.

The form (3.27) shows that I is real, but this is not evident from Eq. (A3). But, by using the canonical form for K , we obtain

$$I = 2 \int_0^{\pi/2} \frac{dx}{(1 - w \cos^2 x - w^* \sin^2 x)^{1/2}}. \quad (\text{A4})$$

If we write $w = a + ib$, expand the integrand in powers of b , and integrate term by term, we obtain

$$\begin{aligned} I &= \frac{\pi}{\sqrt{1-a}} \left[1 - \frac{3}{16} \left(\frac{b}{1-a} \right)^2 + \dots + \frac{(-1)^n}{\pi} \left(\frac{b}{1-a} \right)^{2n} \frac{\Gamma(2n+\frac{1}{2}) \Gamma(n+\frac{1}{2})}{\Gamma(2n+1) \Gamma(n+1)} + \dots \right] \\ &= \frac{\pi}{\sqrt{1-a}} F \left(\frac{1}{4}, \frac{3}{4}; 1; -\frac{b^2}{(1-a)^2} \right), \end{aligned} \quad (\text{A5})$$

where F is the hypergeometric function. This form again shows that I is real. With the Fe_8 parameters, $a = 0.5999$, and $b = 0.6307$. The series (A5) is not convergent for these values of a and b . For efficient numerical evaluation of I in such cases, one can either perform a numerical integration of Eq. (3.27) directly (which is what we did), or reexpress

the hypergeometric function in Eq. (A5) in terms of other hypergeometric functions of the argument

$$\frac{(1-a)^2}{1-2a+(a^2+b^2)} = \frac{(2+P_2)^2}{4(1+P_2+P_4)} \quad (\text{A6})$$

using formula 9.132.1 of Ref. [39]. Since the argument is now small compared to 1 (0.2870 for Fe_8), the hypergeometric series involved are rapidly convergent.

[1] See, e.g., the review by J. Villain: *Molecular Magnetism: A School of Physics*, in *Frontiers of Neutron Scattering*, edited by A. Ferrer (World-Scientific, 2000).

[2] W. Wernsdorfer and R. Sessoli, Science **284**, 133 (1999).

[3] Very recently, oscillatory tunnel splittings have been seen in another molecule dubbed Mn_{12}^{2-} by the authors: W. Wernsdorfer, M. Soler, G. Christou, and D. N. Hendrickson, cond-mat/0109066. This molecule is not yet as extensively studied as Fe_8 , and the authors have analyzed it in terms of the simplest biaxial symmetry model (1.1) given below. If further experimentation confirms fewer than the full number of quenchings predicted by this model, that would be strong indication for a fourth-order anisotropy term similar to that in Fe_8 , and our analysis will apply.

[4] A. Garg, Europhys. Lett. **22**, 205 (1993).

[5] A. Garg, Phys. Rev. Lett. **83**, 4385 (1999).

[6] S. P. Kou, J. Q. Liang, Y. B. Zhang, and F.-C. Pu, Phys. Rev. B **59**, 11792 (1999).

[7] J. Villain and A. Fort, Euro. Phys. J. B. **17**, 69 (2000).

[8] J.-Q. Liang, H. J. W. Müller-Kirsten, D. K. Park, and F.-C. Pu, Phys. Rev. B **61**, 8856 (2000).

[9] S.-K. Yoo and S.-Y. Lee, Phys. Rev. B **62**, 5713 (2000).

[10] A. Garg, math-ph/0003005.

[11] A. Garg, Phys. Rev. B **64**, 094413 (2001); *ibid* **64**, 094414 (2001).

[12] M. Wilkinson, Physica **21D**, 341 (1986).

[13] D. Loss, D. P. DiVincenzo, and G. Grinstein, Phys. Rev. Lett. **69**, 3232 (1992).

[14] J. von Delft and C. L. Henley, Phys. Rev. Lett. **69**, 3236 (1992).

[15] L. D. Faddeev, in *Methods in Field Theory*, Les Houches 1975, edited by R. Balian and J. Zinn-Justin (North-Holland, Amsterdam, 1976).

[16] J. R. Klauder, Phys. Rev. D **19**, 2349 (1979).

- [17] Ersin Keçecioglu and A. Garg, Phys. Rev. Lett **88**, 237205 (2002).
- [18] It should of course be understood that now when we speak of states in which the spin is localized along a particular orientation, there is always a minimum zero-point spread or uncertainty in this orientation. Thus an equation such as $\mathbf{J} = J\hat{\mathbf{z}}$ must be understood as holding for the average $\langle \mathbf{J} \rangle$, and not read literally.
- [19] Ersin Keçecioglu and A. Garg, Phys. Rev. B **63**, 064422 (2001).
- [20] The Hamiltonian (1.4) differs from that in Ref. [2] by a term proportional to \mathbf{J}^2 . This makes no physical difference, since $[\mathbf{J}^2, \mathcal{H}] = 0$. In terms of the parameters D and E of Ref. [2], $k_1 = D + E$ and $k_2 = D - E$.
- [21] D. Gatteschi, A. Caneschi, L. Pardi, and R. Sessoli, Science **265**, 1054 (1994).
- [22] A. L. Barra, P. Debrunner, D. Gatteschi, C. E. Schulz, R. Sessoli, Europhys. Lett. **35**, 133 (1996);
- [23] R. Caciuffo et al., Phys. Rev. Lett. **81**, 4744 (1998).
- [24] M. Hennion et al., Phys. Rev. B **56**, 8819 (1997).
- [25] B. Felsager, *Geometry, Particles, and Fields* (Springer, New York, 1998), Chapter 5.
- [26] A. Garg, Spin Tunneling in Molecular Magnets, cond-mat/0012157.
- [27] The state $|J, J\rangle$ is the usual simultaneous eigenstate of J^2 and J_z with eigenvalues $J(J+1)$ and J , respectively. Hence, $|J, J\rangle = |\hat{\mathbf{z}}\rangle$.
- [28] E. A. Kochetov, J. Math. Phys. **36**, 4667 (1995).
- [29] M. Stone, K.-S. Park, and A. Garg, J. Math. Phys. **41**, 8025 (2000).
- [30] One can also partition the action between ‘kinetic’ and ‘boundary’ terms differently. Following Klauder, e.g., we could write $S_K = -iJ \int \cos \theta d\phi$, and $S_B = J \ln(\sin \bar{\theta}_i \sin \bar{\theta}_f / \sin \theta_i \sin \theta_f)$.
- [31] A. Garg, E. Kochetov, K.-S. Park, and M. Stone, cond-mat/0111139.
- [32] M. V. Berry and M. Wilkinson, Proc. Roy. Soc. Lond. A **392**, 15 (1984).
- [33] The argument that follows has been partially given previously in Ref. 26.
- [34] V. I. Arnold, *Mathematical Methods of Classical Mechanics* (Springer-Verlag, New York, N.Y., 1978). See Appendix 10.
- [35] M. V. Berry, Proc. R. Soc. Lond. A **392**, 45 (1984).
- [36] It should be noted that the expression $\Delta_{1+2} = 2D_1 \cos(J\Phi) \exp(-\text{Re } S_1^{\text{cl}})$ does not hold at the fields we are considering here. As h is increased starting from 0, a value h^* is reached where Φ vanishes, but where the energy still has two minima. The imaginary parts of the two

instantons 1 and 2 are zero for all $h > h^*$. These points known by explicit calculation in the case $C = 0$; see A. Garg, Phys. Rev. B **60**, 6705 (1999).

- [37] For readers who are not happy with this, we offer the following. In stead of fixing the relative signs of Δ_{1+2} at large h , we do so at $h = 0$ (or infinitesimal $h > 0$ for half-integer J). This can be done by computing these amplitudes via perturbation theory in $k_1 - k_2$, C , and h . We leave it to the readers to do this, but similar calculations are given in C.-S. Park and A. Garg, Phys. Rev. B **65**, 064411 (2002).
- [38] The count continues to be correct even in the exceptional case in which the two curves just touch each other, if we regard this as producing a double zero of Δ . The curve of $|\Delta|$ versus h will have a quadratic zero as opposed to the cusps in Figs. 3, 6, or 7.
- [39] I. S. Gradshteyn and I. M. Ryzhik, *Tables of Integrals, Series, and Products*, corrected and enlarged edition (Academic, New York, 1980).